

Discovery of absorption features of the ADC and systematic acceleration of the X-ray burst rate in XB 1323-619

M. J. Church^{1,2}, D. Reed¹, T. Dotani³, M. Bałucińska-Church^{1,2} and A. P. Smale⁴

¹*School of Physics and Astronomy, University of Birmingham, Birmingham B15 2TT, UK*

²*Astronomical Observatory, Jagiellonian University, ul. Orła 171, 30-244 Cracow, Poland*

³*Institute of Space and Astronautical Science, Japan Aerospace Exploration Agency, Yoshinodai 3-1-1, Sagami-hara, Kanagawa 229-8510, Japan*

⁴*Office of Space Science, Astronomy and Physics Division, Code SZ, NASA Headquarters, Washington, DC 20546-0001, USA*

Accepted 2004 December 7. Received 2004 September 17

ABSTRACT

We present results from analysis of the observation of the dipping, quasi-periodic bursting low mass X-ray binary XB 1323-619 made with *XMM-Newton* in Jan., 2003. In spectral analysis of the non-dip, non-burst EPIC PN spectrum, a number of absorption lines were discovered, notably at 6.70 and 6.98 keV which we identify with scattering by high ionization state ions Fe XXV and Fe XXVI. Such features have been seen in other dipping sources, but their origin was not understood. Curve of growth analysis provided a consistent solution in which the line ratio was reproduced assuming collisional ionization with $kT = 45$ keV, close to the electron temperature we previously determined for the accretion disc corona (ADC) in this source. We thus propose that the absorption lines in the dipping LMXB are produced in the ADC. Spectral evolution in dipping was well-described by the progressive covering model which we have previously shown to give very good explanations of many dipping sources. We discuss the proposal of Boirin et al. (2004b), based on analysis of the present observation, that spectral evolution in all of the dipping LMXB may be explained by subjecting the continuum to a highly ionized absorber. This would require a decrease in X-ray intensity by a factor of ~ 3 in dipping at energies where photoelectric absorption is not effective (40 – 100 keV) which previous *BeppoSAX* analysis of several sources firmly rules out. In XB 1323-619, any decrease was less than 10 ± 10 percent, and so the ionized absorber proposal can be ruled out. We find a remarkable linear increase in the rate of X-ray bursts with time over the 14-year period since 1989, and a systematic non-linear increase in source luminosity (L). The linear variation of burst rate with L shows that the burst rate is proportional to mass accretion rate, and if continued implies that the gap between bursts will become zero on January 11, 2008. In reality we expect the source to undergo a transition from X-ray bursting to X-ray flaring which would confirm the suggestion we previously made that flaring is unstable nuclear burning effectively consisting of a superposition of X-ray bursts.

Key words: accretion: accretion discs – binaries: close – stars: neutron – X-rays: binaries X-rays: individual (XB 1323-619)

1 INTRODUCTION

XB 1323-619 is a member of the class of dipping low mass X-ray binaries (LMXB) exhibiting absorption dips at the orbital period, and is also remarkable as one of the very few X-ray burst sources in which the bursts occur regularly, but not quite periodically. The dipping is due to absorption in the bulge in the outer accretion disc (White & Swank 1982; Walter et al. 1982). Spectral evolution in dipping in these sources

provides a powerful tool for constraining emission models for LMXB since not only non-dip emission but also several levels of dipping must be fitted. In recent years, we have shown that the complex spectral evolution in dipping can be explained in terms of absorption of two components: blackbody emission of the neutron star and Comptonized emission from a very extended Accretion Disc Corona (Church & Balucinska-Church 1993, 1995; Church et al. 1997, 1998a).

The gradual removal of the non-thermal emission in dipping shows that the ADC must be extended. Identification of the continuum emission with the above sources was strongly confirmed by the measurement of dip ingress times, for almost all of the dipping sources, using data from several satellites (Church & Bałucińska-Church 2004). This showed that the size of the ADC varies with X-ray luminosity between 20,000 km and 500,000 km or between 6–60 percent of the accretion disc radius. This very large size rules out the possibility that the Comptonized emission originates in a small central region around the compact object as has often been assumed (Oosterbroek et al. 2001; Sidoli et al. 2001; Gierlinski & Done 2002). In addition, there are many arguments based on observational evidence that the thermal component is from the neutron star and not the inner disc (Barnard et al. 2003); for example, the smooth merging of the thermal emission between X-ray bursts and the quiescent source, and the fact that an extended ADC will cover the inner hot disc, Comptonizing the emission, so that disc blackbody will not be seen. Investigation of line emission variation in dipping can indicate the source of the line. In XB 1916-053, a line at 0.65 keV varies in dipping in exactly the same way as the Comptonized emission showing that the line must originate in the ADC (Church et al. 1997). In recent years, absorption features have been discovered in several sources, notably the galactic jet source GRS J1915+105 (Kotani et al. 2000), in the LMXB GX 13+1 (Ueda et al. 2001) and in the dipping LMXB, such as XB 1916-053 (Boirin et al. 2004a). As X-ray dips are seen in the jet source and also in GX 13+1, it is clear that the absorption features are related to the high inclination of these systems, although the exact location of the absorber has not been identified. It thus seems likely that all dipping sources will exhibit absorption features which can be used as diagnostics of plasma parameters in the absorbing region.

XB 1323-619 was found using *Uhuru* and *Ariel V* (Forman et al. 1978; Warwick et al. 1981), and dipping at the orbital period of 2.93 hr and X-ray bursting were discovered using *Exosat* by van der Klis et al. (1985). During the *Exosat* observation, the bursts repeated on a timescale of 5.30 – 5.43 hr, approximately on every second orbital cycle. Spectral evolution in dipping was modelled using the “absorbed + unabsorbed approach” (AU) by Parmar et al. (1989), also applied to other dipping sources (Courvoisier et al. 1986; Smale et al. 1988) in which the non-dip spectral model is split into two parts for dipping. Dip spectra can be fitted if one part is absorbed, while the other is not absorbed but requires normalization decreasing by up to 10 times; however, this approach is difficult to justify physically. Moreover, broadband spectra of dipping sources with *BeppoSAX* provide an unambiguous test of the AU approach, since if the large decrease in normalization necessary to fit dip spectra in the band 1 – 10 keV is real, then the spectra in the range 40 – 100 keV should also exhibit a vertical shift downwards by a large factor. It is quite clear from the *SAX* observations of XB 1323-619 (Bałucińska-Church et al. 1999; hereafter BC99) and XB 1916-053 (Church et al. 1998b) that there is *no* such decrease, and this is strong evidence against the AU approach. Thus although the absorbed + unabsorbed approach may *appear* to explain spectral evolution in instruments not extending above 10 keV, it *totally fails to explain dipping in the band 0.1 – 300 keV*.

An explanation of spectral evolution in dipping known as the progressive covering model was proposed more recently (e.g. Church et al. 1997) which takes into account the strong evidence for an extended ADC, so that the absorber gradually overlaps larger fractions of the ADC. At any stage, a fraction of the ADC remains uncovered giving an unabsorbed fraction of the spectrum which decreases as dipping deepens, thus explaining the need for a decreasing normalization in the AU approach. The covered part of the ADC provides an absorbed part of the spectrum, while the neutron star blackbody is rapidly absorbed once the point source is overlapped by absorber. This progressive covering approach is clearly more physical, and has given extremely good fits to dip spectra in many sources using a range of satellite observatories (Church 2001). More important, it explains dipping in broad energy bands, such as that of *BeppoSAX*, i.e. in the region 10 – 100 keV, which the absorbed and unabsorbed approach is unable to do, which therefore must be rejected as incorrect.

XB 1323-619 was observed by us with *BeppoSAX* 1997, August 22 (BC99) and using *Rossi-XTE* on 1997, April 25 (Barnard et al. 2001). The *BeppoSAX* observation allowed a detailed study of the X-ray spectrum, and of dipping and bursting. The broadband spectrum in the range 1–200 keV allowed accurate determination of emission parameters, and the relatively high cut-off energy of 44 keV of the Comptonized emission, ten times higher than in many LMXB, proves a high electron temperature in the ADC. The neutron star blackbody emission had $kT = 1.77 \pm 0.25$ keV contributing ~ 15 percent of the 2 – 10 keV flux. Spectral analysis of a burst that took place during a dip interval exhibited a surprising lack of absorption shown to be consistent with ionization of the absorbing bulge by the X-ray burst (BC99), showing that during the burst *all* of the accretion disc must be highly ionized. The *RXTE* observation giving 100 times improved count statistics could not be fitted without including the effects of dust scattering, and the optical depth to dust scattering was obtained from the radial intensity profile of the *BeppoSAX* data (Barnard et al. 2001). The *RXTE* observation also revealed a broad iron emission line at 6.43 ± 0.21 keV with equivalent width (EW) 110 ± 55 eV.

During the above observations, it was seen that the burst rate was increasing; for example in the *BeppoSAX* observation the bursts were repeating every 2.40 – 2.57 hr. Although this might be expected to be due to changes in mass accretion rate, i.e. source luminosity, there was at this stage no apparent systematic change in the luminosity. The source luminosity (1 – 10 keV) was $\sim 2 \times 10^{36}$ erg s⁻¹ entirely consistent with the observation of X-ray bursts which are seen in lower luminosity sources, but not in brighter LMXB closer to the Eddington limit which exhibit X-ray flaring.

In the present paper, we present analysis results for our observation of the source with *XMM-Newton* in which several absorption features were discovered. In addition, we find that the burst rate has increased substantially, and we can now show that this is very well correlated over a period of 14 years with a systematic increase in the source luminosity, presumably reflecting an increase in mass accretion rate from the Companion, the reason for which is not clear.

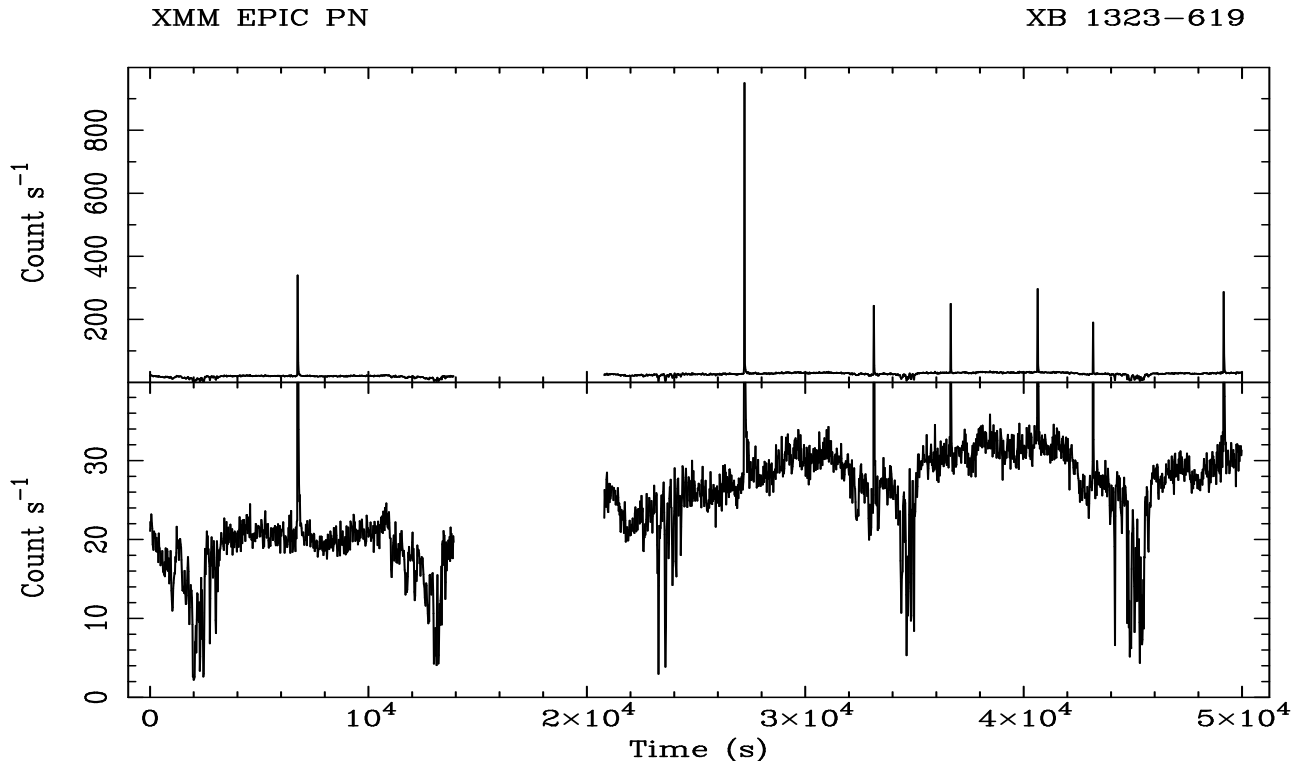


Figure 1. EPIC PN lightcurve of XB 1323-619 in the band 0.5–10.0 keV: lower panel shows the X-ray dipping; the upper panel shows the X-ray bursts more clearly with burst heights corrected (see text)

2 OBSERVATIONS AND ANALYSIS

We observed XB 1323-619 on 2003 Jan 29 from 09:03 – 22:47 UT for a total observation of 50 ks containing a usable exposure of 43 ks. The European Photon Imaging Cameras (EPIC) consist of two MOS and one PN spectrometer. Because the PN instrument is effectively two times more sensitive than the MOS as it diverts no flux to the grating instruments, we present PN results here. Raw data were assembled into events files which were then used to provide lightcurves, images and spectra using the Science Analysis Software SAS, version 5.4.1. Hot and flickering pixels and the neighbouring pixels of these were removed during the processing. Standard processing was used so that CCD events in single or double pixels produced by a single photon were accepted and other events rejected. There was no pulse pileup effect as the count rate even at the peak of the largest X-ray burst was well below that at which pileup is first seen. Barycentric correction was carried out, and finally, during a period of high particle background from 13.9–20.8 ks, science data were not accumulated.

The PN detectors were operated in timing mode in which only a single CCD containing the source is used, and image data were not available since the data are projected onto one dimension. The field of view of the single chip is 199×64 pixel, where 1 pixel is $4.1''$ i.e. $13.6' \times 4.4'$. We extracted source events from a column $70''$ wide centred on the source position, and obtained background from two columns each $35''$ wide at the edges of the strip, each $\sim 115''$ from the source. The field of view of the detector was such that the X-ray pulsar discovered during the *BeppoSAX* observation of XB 1323-619 (Angelini et al. 1999) and located $17'$ away, was

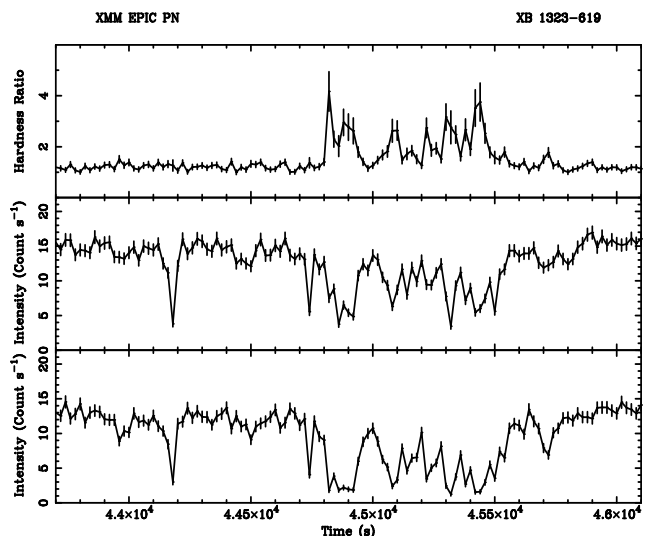


Figure 2. Detailed view of the 5th dip in two energy bands: centre panel: 0.5–3.5 keV, lower panel: 3.5–10 keV together with the hardness ratio formed from dividing these (top panel). The marked spectral hardening in dips can be seen, except for the unusual events at the start of dipping (see text)

not included and could not contaminate the data. The latest instrument response file for the PN (epn_ti40_sdY9.rsp) released in January, 2003, was used.

3 RESULTS

The background-subtracted X-ray lightcurve obtained from the EPIC PN in the energy range 0.5 – 10 keV is shown in Fig. 1 with 20 s binning (lower panel). 5 intervals of dipping can be seen, and the 7 X-ray bursts are displayed separately in the upper panel. Two of the bursts occur in the wings of X-ray dips, although no bursts coincide with deep dipping. With 20 s binning, bursts do not have their true height and so we examined each burst individually with shorter binning, decreasing the bin size until at a few seconds, there was no change in burst height. The bursts are shown for clarity separately in the upper panel of Fig. 1 with corrected heights. It is striking that one burst is very much more intense than the others with peak intensity 35 times that of the persistent emission, about 3 times larger than the other bursts. The two bursts coinciding with the wings of X-ray dips are slightly reduced in intensity compared with the other bursts. The mean interval between bursts in the second half of the observation containing 6 bursts is 58 min. However, in the first part of the observation only one burst is seen when 3 might have been expected, and there is more variation in burst height, suggesting that the bursting is rather more erratic than previously, e.g. in *BeppoSAX*, possibly associated with the increased source luminosity (Sect. 3.3).

Dipping is deep, the intensity falling by 85 percent of the non-dip value and exhibits a high degree of variability. The data were searched for periodicities to obtain a measurement of the orbital period from the dip recurrence using the FTOOL POWSPEC and a period of 2.980 ± 0.053 hr obtained with PN data, and 2.961 ± 0.048 hr with MOS. The average of these is 2.97 ± 0.05 hr which is consistent with the period obtained from *BeppoSAX* of 2.938 ± 0.020 hr (BC99). In Fig. 2 we show an expanded view of the variability in the fifth dip, together with the associated increase in hardness ratio, defined as the intensity in the band 3.5–10 keV divided by that in the band 0.5–3.5 keV. The deep dipping within the dip envelope displays increases in hardness as expected; however the first two dip events have no associated hardening, which is very unusual. We examined the lightcurves in the bands 0.5–3.5 and 3.5–10.0 keV and found these dip events to have exactly equal depth. The only exception previously found to the photoelectric absorption that produces X-ray dips, is the occurrence of electron scattering in the “shoulders of dipping” in the brighter dip sources X 1624-490 and XB 1254-690 (Smale, Church & Bałucińska-Church 20001, 2002), i.e. when the lightcurves display dipping at about the 10 percent deep level before deep dipping starts, which we have explained as electron scattering in the outer highly ionized layers of the absorber. This is not seen in conjunction with fast variability in dipping which is due to absorption of the point-like neutron star emission. Thus it appears that this event is caused by the neutron star emission being either fully absorbed by very dense matter or reduced by electron scattering in fully ionized material probably on the outer disc.

In the band 0.5–2.0 keV, dipping is 100 percent deep, showing firstly that the absorber subtends a larger angle at the neutron star than the extended emission component. This deep dipping is also initially surprising in view of the dust scattering previously found with this source. For sources with higher Galactic column densities, scatter-

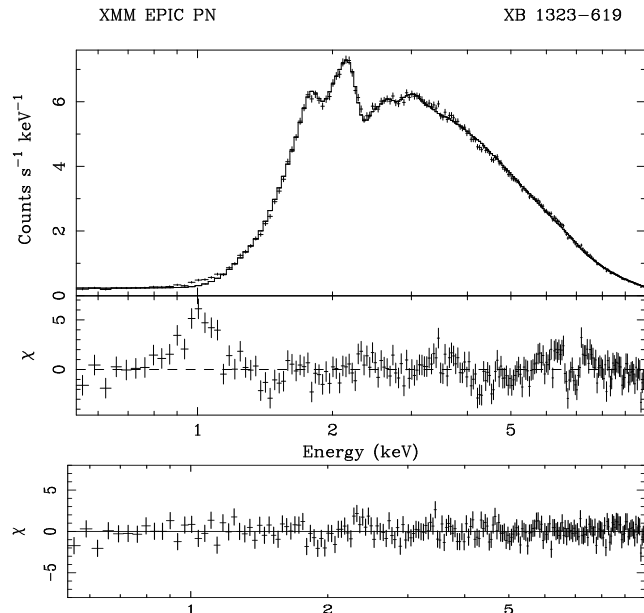


Figure 3. Spectral fit of the non-dip, non-burst spectrum. The upper panel shows the folded data and residuals before addition of lines to the spectral model, while the lower panel shows the residuals after the lines were added

ing takes place both out of and into the beam. Because of the delay involved in the scattering process, a fraction of the non-dip emission is added to the dip intensity reducing the observed depth of dipping. Thus in the observations of XB 1323-619 with *BeppoSAX* (BC99) and *RXTE* (Barnard et al. 2001) the depth of dipping did not reach 100 percent although other factors also contributed to this. In the case of *BeppoSAX*, data were extracted from circular regions around the source of radius $4'$ for the MECS, while in *RXTE*, no selection was possible as the PCA is not imaging. It was concluded that the dust scattering halo contributed a few percent in the case of *RXTE*, this having been derived from fitting the radial intensity profile in *BeppoSAX*, so that dipping could never be 100 percent deep. We investigated dust scattering in the present *XMM* observation by re-binning the MOS image into radial bins in the range 0.5 to 300 arcseconds, and comparison of this with the point spread function reveals a clear excess above the PSF at $r > 40''$ which can be identified with the dust scattering halo. However, data selected for analysis were obtained from a region of size $35''$ and hence dust scattering does not prevent dipping becoming 100 percent deep.

3.1 The EPIC PN spectrum of persistent emission

Non-dip, non-burst intervals of data were selected from the lightcurve of XB 1323-619, and to obtain the best spectrum for detection of lines, the whole observation was used (excluding bursts) although there was a 50 percent increase in luminosity during the observation. In analysis of dipping, only data from the second half of the observation were used where the intensity was stable to avoid mixing data of different intensities. In our previous work, we have shown that the continuum spectra of the dipping LMXB, and indeed of LMXB in general, can be best-fitted by a two-component

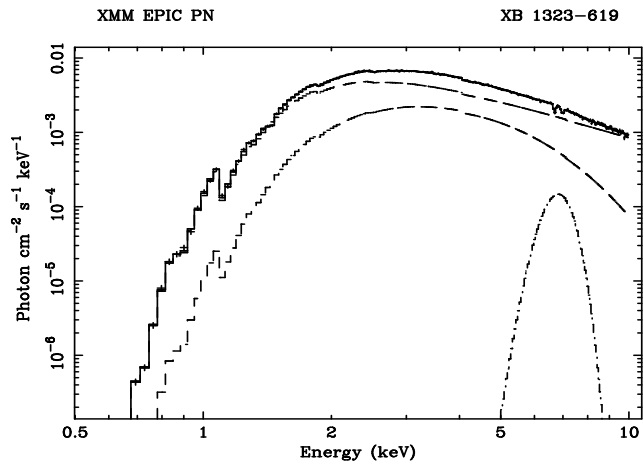


Figure 4. The unfolded non-dip, non-burst spectrum with best-fit model consisting of continuum plus line and edge features

model consisting of blackbody from the neutron star and Comptonized emission from an extended ADC (Sect. 1). In the high quality, broadband *BeppoSAX* data on XB 1323-619 this was also the case (BC99). For this reason, we apply the above continuum model to the above data as the evidence for it is so strong. We note that in analysis of *XMM* data on other dipping sources, Parmar and co-workers (e.g. Boirin et al. 2004a) choose a model containing a disc blackbody component although there is little evidence to support this.

Primitive channels were binned together such that, at any energy, the energy resolution was oversampled by a factor of three; in addition the data were grouped to a minimum of 20 counts per bin so that the χ^2 statistic could be used. Systematic errors of 2 percent were added. Data were fitted in the band 0.52–10.0 keV, so avoiding a point at 0.5 keV which appeared anomalous. Fig. 3 shows the folded spectrum of the persistent emission fitted by a continuum model only, together with the residuals, from which it is immediately clear that various absorption and emission features were present. Firstly, there is a broad feature at ~ 1 keV. This can be fitted either by an emission line or by an absorption edge. A comparison of χ^2 values can best be made when all other absorption and emission features are added, and at that stage, there is no significant difference in goodness of fit of emission line or edge. If an emission line is used, the energy is 0.80 keV corresponding to Fe XXVII or O VIII although the line is broad and very strong (EW ~ 4 keV), and without apparent structure. The energy appears higher in Fig. 3 because the line is modified by absorption. An edge at ~ 1.1 keV could consist of Ne VII (1.078 keV), Ne VIII (1.125 keV), Fe XIII (1.081 keV) or Fe XIV (1.125 keV). We choose to adopt the edge model, because of the possibly unreal width and strength an emission line would need. However, there is evidence from dip spectra (below) marginally against the edge model: when we added the two lowest dip levels together to obtain a spectrum extending down to 0.5 keV, but with only two bins spanning 0.6–1.5 keV. Although the spectrum at 1 keV was of poor quality, there was no sign of any feature at 1 keV. While we expect an emission line to be absorbed in dipping, an edge would probably not be removed. Thus the edge nature of the 1 keV feature cannot be regarded as quite definite.

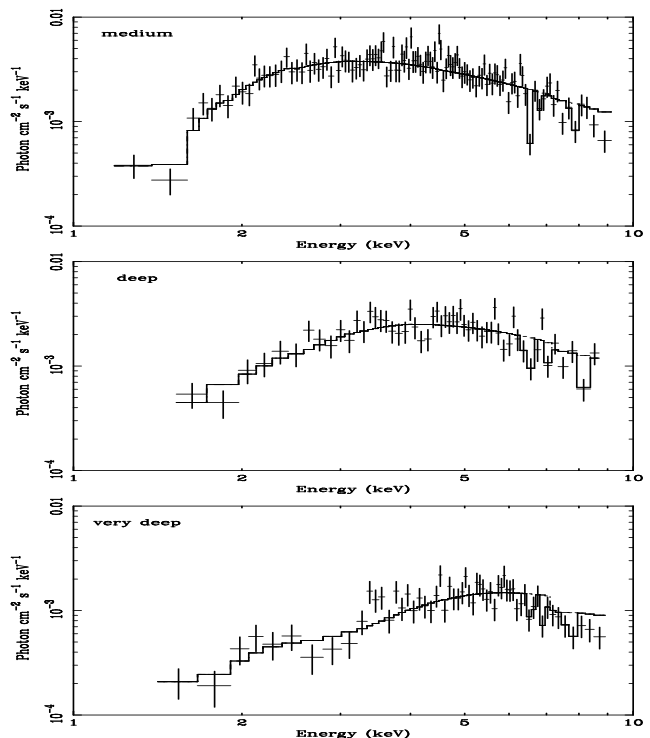


Figure 5. Spectra of three levels of dip emission showing that the progressive covering model provides very good fits to the continuum at all levels.

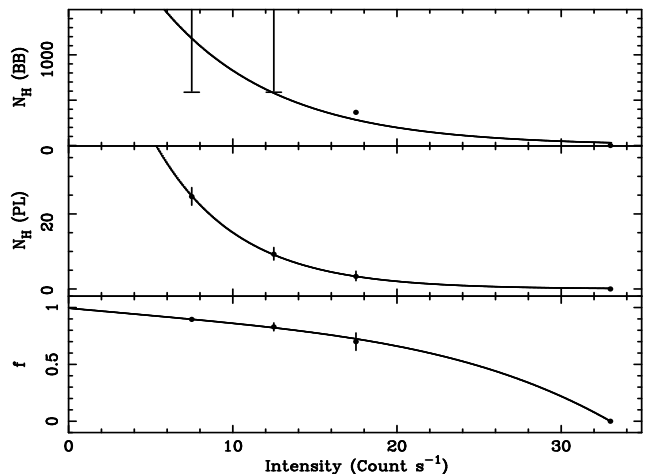
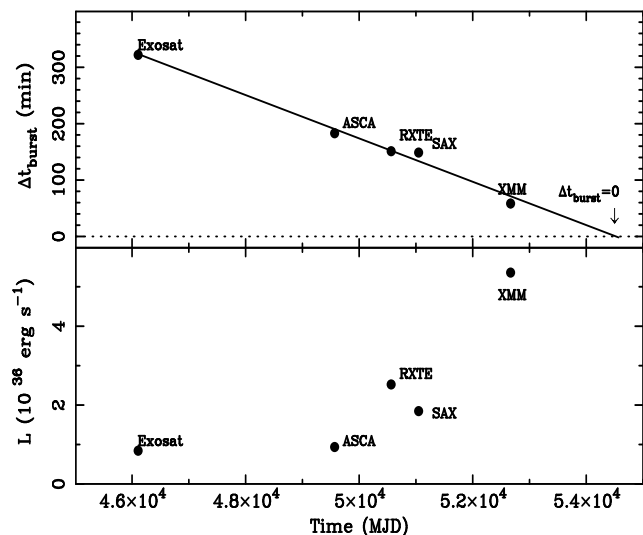


Figure 6. Best-fit spectral fitting results : variation of blackbody column density, power law column density and power law partial covering fraction f with intensity. N_H is in units of 10^{22} H atom cm^{-2}

Using the edge model, a number of absorption features can be seen in the residuals, notably the lines at 6.70 keV and 6.98 keV (Fe XXV and XXVI). There was also a weak feature at ~ 1.46 keV which might correspond to Mg XII, but an EW of a few eV does not constitute a significant detection. There was also some sign of weak, narrow absorption at 7.8 keV corresponding to Ni XXVII. A feature at 4.0–4.6 keV could be fitted as an absorption line or as an edge. If fitted as a line, the energy obtained of ~ 4.6 keV does not correspond to a known line, but an edge at ~ 4.0 keV may be Ca XX. Starting from the continuum-only fit,

Table 1. Line and possible edge features detected in the non-dip spectrum of XB 1323-619. In the case of the emission line, the measured energy may have been affected by the neighbouring absorption lines, and identification of the transition is uncertain

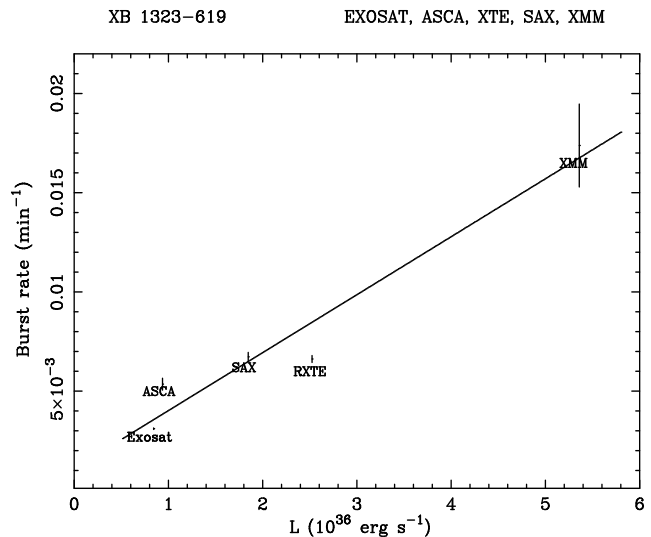
E (keV)	Em/Abs	EW (eV)	F-test prob.	Transition	Energy (keV)
1.09 ± 0.01	edge	...	3×10^{-23}	Ne VII/VIII, Fe XIII/XIV	1.08, 1.13, 1.08, 1.13
1.46 ± 0.03	A	-15	1×10^{-4}	Mg XII	1.48
4.05 ± 0.08	edge	...	1×10^{-6}	Ca XX $K\alpha$	4.03
6.70 ± 0.03	A	-22	2×10^{-7}	Fe XXV $K\alpha$	6.68
6.98 ± 0.04	A	-27	1×10^{-6}	Fe XXVI $K\alpha$	6.95
6.82 ± 0.11	E	92	3×10^{-6}	Fe XXV/XXVI	6.68/6.95

**Figure 7.** Top panel: the long-term variation of the mean interval between bursts, fitted by a linear model; Δt errors, typically ± 5 min, are too small to be seen. Lower panel: the 1–10 keV source luminosities for each of the observations

lines were added to the spectral model sequentially, until the final model was obtained having the lines shown in Table 1. The best-fit is shown in Fig. 4 as an unfolded spectrum, and the remaining small residuals shown in Fig. 3 (lower panel). From these, it can be seen that the broad positive residuals between 6–8 keV in the continuum model were partly a result of the absorption features not being modelled; in the final fit, this resolves itself into a single emission line, although the measured energy of 6.8 keV was probably distorted by the neighbouring absorption lines, making identification uncertain. The interpretation of these features is discussed in Sect. 4. The best-fit values of the continuum parameters were $kT = 1.09^{+0.07}_{-0.02}$ keV for the neutron star blackbody, power law photon index $\Gamma = 1.69 \pm 0.08$, and the column density N_{H} was $2.42 \pm 0.14 \times 10^{22}$ atom cm^{-2} . The column density is somewhat larger than the Stark et al. (1992) value of $\sim 1.4 \times 10^{22}$ atom cm^{-2} .

3.2 Spectral evolution in dipping

Dip spectra were produced by selecting in intensity bands from the second half of the observation. X-ray bursts were removed, and intensity bands defined of 5–10, 10–15, 15–20 count s^{-1} for deep, medium and shallow dipping, and also the non-dip spectrum at 30–36 count s^{-1} . The non-dip

**Figure 8.** The data of Fig. 7 re-plotted as $1/\Delta t$, i.e. as burst repetition rate as a function of L^{1-10} with best-fit simple linear model

spectrum contained only data from times later than 30 ks in the observation, to exclude earlier data at lower intensity. This spectrum was fitted to obtain the emission parameters: N_{H} , kT , Γ and the normalizations, and these were frozen in fitting the dip spectra as only absorption parameters can change. The same line and edge features as found above were included in fitting each spectrum. The spectral model tried in fitting had the form $\text{AG}^*(\text{AB}^*\text{BB}+\text{PCF}^*\text{PL})$, where AG is Galactic absorption, BB is the neutron star blackbody emission, AB the absorption of the blackbody and PL is the Comptonized emission of the extended ADC. The point-like blackbody is allowed to be covered rapidly once the envelope of the absorber passes across the neutron star, but the ADC is subject to progressive covering modelled as PCF: a partial covering fraction as the absorber progressively overlaps more of the ADC. This “progressive covering” model (Sect. 1) has previously provided very good fits to observations of the dipping sources, including XB 1323-619 (Church et al. 1997; BC99).

Good fits were obtained for the dip spectra with the emission parameters frozen at the non-dip values, with $\chi^2/\text{d.o.f.} = 104/101$, 46/40 and 57/45, for medium, deep and very deep dipping, and these fits are shown in Fig. 5 where simple fits are added to the data. Clearly the two deeper dip spectra are not of the highest quality because of the lack of counts. The variation of the absorption parameters within

the progressive covering model are shown in Fig. 6. It can be seen that the covering fraction rises smoothly from zero to 95 percent in the deep dip spectrum, and that the column density is much higher for the neutron star blackbody emission than for the extended emission, and only lower limits can be given for the lower two dip levels. The reason that this column density is higher is that the neutron star effectively allows measurement of N_{H} along a line through the centre of the absorber, whereas the extended emission has N_{H} determined as an integration over the absorber including lower density outer regions. It is quite clear that the above absorber modelling gives good fits, providing further evidence for the progressive covering model which gives a clear physical explanation of spectral evolution in dipping, and thus evidence against the alternative “absorbed plus unabsorbed” approach.

The absorption lines of the non-dip spectrum were found to become more pronounced in dipping, in particular the Fe XXV and XXVI lines. In addition, it was striking that an additional absorption line at ~ 7.8 keV corresponding to Ni XXVII K_{α} was clearly detected, which although just seen in the non-dip spectrum, did not constitute a significant detection. The equivalent width of the Fe XXV line in the deep dip spectrum was ~ 100 eV, that is, five times larger than in the non-dip spectrum. The increase in EW reflects an increase of integrated flux in the line in dipping by a factor of 2.5 compared with non-dip, while the continuum spectral flux density decreases by a factor of two, thus there is clearly additional absorption in the line. The relatively poor statistics of the dip spectra tended to mask systematic trends in the line parameters; however, the Fe XXV line energy in the dip spectra was 6.55 ± 0.1 keV. This is consistent with a decrease of the ionization state of the additional absorber involved in forming absorption lines in dipping. Finally, the strong emission line at ~ 6.8 keV was not present in the dip spectra implying that this was produced in the ADC so that in dipping it is removed as the ADC is overlapped by absorber.

3.3 14-year acceleration increase of rate of X-ray bursts

We next present results on the clear systematic change of X-ray burst rate over the 14-year interval since the *Exosat* observation. For the *RXTE*, *ASCA* and *SAX* observations, we use our previously published burst rates (Barnard et al. 2001; BC99); for *Exosat* we also use the published rate (Parmar et al. 1989). In the case of the *Exosat*, *RXTE* and *SAX* observations, the bursting clearly displayed the regularity for which the source is known, i.e. most bursts repeated regularly. However, in obtaining the mean burst separation, we did exclude bursts following double bursts which cause a glitch in the burst repetition rate. In the *XMM* observation, it appears that the degree of regularity has decreased presumably associated with the luminosity increase. Thus Fig. 1 shows that in the second half of the observation, the bursts tend to be regular, but this is not seen in the first half. Consequently, we make the best estimate possible from the second half. This value of 58.4 ± 7 min between bursts is remarkably shorter than in previous observations of this source. In *Exosat* (1985, February) the separation was 5.30 – 5.43 hr (Parmar et al. 1989), in *ASCA* (1994, August) it was 3.05 hr

Table 2. Column densities of absorbing ions for the non-dip spectrum from curve of growth analysis shown as logarithms. Also shown are implied values of kT_{therm} if the ion distributions are due to collisional ionization, and values of the ionization parameter ξ for ions produced by photo-ionization. For each ionization process, the hydrogen column density of the plasma is given in non-logarithmic form

specie	$kT_{\text{CG}} = 100$ keV	$kT_{\text{CG}} = 45$ keV	$kT_{\text{CG}} = 1$ keV
Fe XXV K_{α}	17.6 ± 0.1	17.8 ± 0.1	18.7 ± 0.2
Fe XXVI K_{α}	18.0 ± 0.1	18.8 ± 0.1	19.95 ± 0.1
thermal ionization			
N_{H} (atom cm^{-2})	9.9×10^{22}	1.7×10^{24}	2.7×10^{25}
kT_{therm} (keV)	14	42	100
photo-ionization			
N_{H} (atom cm^{-2})	4.3×10^{22}	4.0×10^{23}	8.0×10^{25}
ξ (erg cm s^{-1})	$10^{3.4}$	$10^{3.6}$	$10^{4.3}$

(BC99); *XTE* (1997, April) it 2.45 – 2.59 hr (Barnard et al. 2001) and in *BeppoSAX* (1997, August) it was 2.40 – 2.57 hr (BC99). Thus it is very clear that the rate of bursting has been increasing systematically since 1985 and probably before that.

To investigate the dependence of burst rate with source luminosity, we have compiled the values of source luminosity from our spectral analysis of the *ASCA*, *RXTE* and *BeppoSAX* observations. In addition we obtained the *Exosat* ME spectrum and instrument response from the HEASARC archive and carried out spectral fitting of this using the same two-component model used with the other observations (see Sect. 3.1). In all cases we derived the flux and luminosity in the 1 – 10 keV band, assuming a distance of 10 kpc, to avoid extrapolating too far from the actual instrumental energy ranges. The results are shown in Fig. 5 in the form of burst recurrence time Δt as a function of MJD (upper panel), and source luminosity L (lower panel). The linear variation of burst rate is remarkable, and is presumably due to the systematic increase of luminosity over the 14 year period covered. It should be noted that the data from *Exosat*, *RXTE* and *SAX* by themselves prove the change in burst rate; the *XMM* data are clearly consistent with this trend, even if the regularity of the bursting had decreased. Least squares fitting of the data in Fig. 5 produced a best-fit linear slope of -0.03847 min MJD^{-1} such that if we assume the linear behaviour continues, the gap between bursts would become zero on MJD 54476, i.e. on 2008, Jan 11. In reality, we do not expect this to happen, since only low luminosity sources exhibit X-ray bursts while brighter sources exhibit flaring; thus we expect the source to undergo a gradual transition to flaring before 2008 as the luminosity increases from 10^{37} to 10^{38} erg s^{-1} .

We also plotted $1/\Delta t$ as a function of L to test the hypothesis that the burst rate is increasing because of the luminosity increase: for a given mass accretion rate \dot{M} , the gap Δt is determined by the time to accumulate sufficient mass on the neutron star surface for a nuclear event. Thus with increasing L and \dot{M} , $1/\Delta t$ should be proportional to L . Fig. 6 shows that this is indeed the case, with a simple linear fit added to the data. This source is remarkable in having burst rate $\propto \dot{M}$ as also found recently for the other quasi-

periodic burster GS 1826-238 by Galloway et al. (2004). Although this may be expected theoretically, the majority of burst sources have a burst rate that *decreases* with increasing \dot{M} (e.g. Strohmayer & Bildsten 2003), perhaps because the burning area increases so that the mass flow per unit area may decrease.

4 DISCUSSION

Fitting the spectra of XB 1323-619 has shown that both the emission model used, and the progressive covering absorption model provide very good fits. Thus the non-dip continuum spectrum is well-described by assuming blackbody emission from the neutron star plus Comptonized emission from the extended accretion disc corona. Fig. 5 shows that the absorption model provides excellent fits to several levels of dipping, this model assuming that the extended ADC is covered gradually by the extended absorber, so that at every stage of dipping, part of the ADC is covered by absorber and part is not. This progressive covering explanation of spectral evolution in dipping has been shown to explain dipping in many dipping sources, and crucially, is able to explain dipping in broadband X-ray observatories such as *SAX*, i.e. it predicts that *no* change will take place in the range above 40 keV where there is no photoelectric absorption, in agreement with observation (see Sect. 1). “Absorbed plus unabsorbed” modelling which was previously used predicts an intensity decrease of typically a factor of 10 above 40 keV which is definitely not seen and the model must be rejected as incorrect.

Analysis of the present observation by Boirin et al. (2004b) claims that both continuum evolution in dipping and the absorption lines could be modelled by an ionized absorber, and that this might be able to explain *all* LMXB dipping sources. A consequence would be that an extended ADC would not be required. However, this suggestion can be ruled out. Firstly, they ignore the strong evidence from dip ingress timing (Church & Bałucińska-Church 2004) that the dominant Comptonized emission region (the ADC) is very extended, as well as evidence cited in many papers (see Sect. 1) that one emission component is removed gradually in dipping showing that it must be extended. The use of an ionized absorber model means a high degree of electron scattering of the continuum *which we can rule out*. Their ionized absorber has ionization parameter $\log \xi \sim 4.0$ (non-dip) and 3.5 (deep dipping) so that almost all electrons are removed from ions. Their ionized absorber column density in deep dipping is equivalent to an electron column density N_e of $1.8 \times 10^{24} \text{ cm}^{-2}$. In non-dip emission, the value is ~ 100 times less. Thus the increase of electron column density in dipping would cause a decrease in X-ray continuum intensity at every energy due to Thomson scattering by a factor of $\exp(-N_e \sigma_T)$ where σ_T is the Thomson cross-section, equal to 3.2. But the high energy spectra of several dipping LMXB in the *SAX* PDS instrument have already been examined, including that of XB 1323-619 (BC99) in which the change in intensity in the 20 – 50 keV PDS band was $< 10 \pm 10$ percent. Thus it is clear that the continuum components *are not subject to ionized absorber*, and so we can rule out the proposed model for the dipping LMXB based on ionized absorber.

The detection of several absorption features in the non-dip spectrum of XB 1323-619, notably those of Fe XXV K_α and Fe XXVI K_α allows derivation of column densities for these species and for consideration of the site of the absorption. We use the curves of growth for these transitions obtained by Kotani et al. (2000) in which equivalent widths are given as a function of column density for a range of plasma temperatures between 0.1 and 1000 keV. In our case, the best-fit values are $\text{EW} = 22 \pm 3 \text{ eV}$ for Fe XXV K_α , and $27 \pm 4 \text{ eV}$ for Fe XXVI K_α . Using the curves of growth, we convert these to column densities as shown in Table 2 for three values of the temperature used in curve of growth calculations kT_{CG} : 100 keV, 45 keV and 1 keV. We will consider the two possibilities that the absorbing plasma is formed by collisional ionization or photo-ionization.

For collisional ionization, we will find the plasma thermal temperature kT_{therm} needed to give the observed ratio of column densities for Fe XXVI and Fe XXV. Using published data on the distribution of ionization states of iron with kT_{therm} (Makishima 1986), we obtain $kT_{\text{therm}} = 14 \text{ keV}$ for $kT_{\text{CG}} = 100 \text{ keV}$, and $kT_{\text{therm}} = 100 \text{ keV}$ for $kT_{\text{CG}} = 1 \text{ keV}$. Assuming that all of the iron in the plasma is in the forms Fe XXVII, Fe XXVI or Fe XXV, we can easily obtain the density fraction of Fe XXV. Then, assuming solar abundances, i.e. that the ratio $\text{H/Fe} = 3.02 \times 10^4$, and using the measured column density of Fe XXV we find the overall plasma column density N_{H} . For example, for a curve of growth temperature $kT_{\text{CG}} = 100 \text{ keV}$, a value N_{H} of $9.9 \times 10^{22} \text{ atom cm}^{-2}$ follows. However, for a low curve of growth temperature of 1 keV, N_{H} becomes very high at 2.7×10^{25} (see Table 2). This latter possibility can be rejected since the degree of electron scattering in this plasma would be very high with a reduction in X-ray intensity by a factor $\exp(-N_e \sigma_T) = \exp(-16)$. Thus X-rays would be very strongly attenuated at all energies by Thomson scattering, and the source luminosity would be many orders of magnitude greater than the apparent value, many times brighter than any Galactic LMXB.

Similarly, we have obtained N_{H} values assuming photo-ionization. In this case we use ion distributions as a function of the ionization parameter ξ (Kallman & McCray 1982; Makishima 1986), and find that values of $\xi = 2500$ and 20000 erg cm s^{-1} are needed for $kT_{\text{CG}} = 100 \text{ keV}$ and 1 keV respectively. For these, the corresponding column densities N_{H} are 4.3×10^{22} and $8.0 \times 10^{25} \text{ atom cm}^{-2}$ respectively. Again, we may reject the very high column density case.

The problem in interpreting the curve of growth analysis is to identify the curve of growth temperature kT_{CG} with a real plasma temperature. There are several possible temperatures, firstly a thermal value kT_{therm} and an ionization temperature kT_{ioniz} . For collisional ionization, there would be thermal equilibrium with $kT_{\text{CG}} = kT_{\text{therm}}$. For photo-ionization, kT_{ioniz} would determine the distribution of ion types, with $kT_{\text{CG}} = kT_{\text{ioniz}}$ which can differ from kT_{therm} . There may also be a third temperature as suggested by Kotani et al. (2000) characteristic of a bulk motion such as an outflow or of turbulence. For both ionization processes, we can reject a low curve of growth temperature of $\sim 1 \text{ keV}$. If we argue that kT_{CG} must be of the order of 100 keV to avoid N_{H} becoming large implying strong Thomson scattering, we are faced with the problem that kT_{CG} is inconsistent with the required kT_{therm} of 14 keV and would conclude that

photo-ionization must operate with kT_{CG} equal to a third plasma temperature reflecting an unknown process.

However, this can be avoided for a curve of growth temperature of 45 keV, also shown in Table 2. For collisional ionization this requires $kT_{\text{therm}} = 42$ keV and so is consistent. N_{H} is 1.7×10^{24} atom cm^{-2} for which the reduction by electron scattering is $\exp(-1.0)$, i.e. by three times. This is not so high that we can reject this possibility. For photo-ionization the N_{H} value is also relatively low. However, both $kT_{\text{therm}} = 42$ keV and $\xi = 4000$ appear to be inconsistent with conditions on the outer accretion disc. However, a temperature of ~ 42 keV is consistent with the range of values we have previously obtained for the electron temperature of the ADC in this source. The broadband *BeppoSAX* spectrum of XB 1323-619 allowed a Comptonization cut-off energy of $44.1_{-4.4}^{+5.1}$ keV to be measured (BC99). The electron temperature depends on the optical depth τ with $kT_e = E_{CO}$ for low τ , and $3 kT_e = E_{CO}$ for high τ . This gives $kT_e = 13$ keV (high τ) and 44 keV (low τ). However, the measured ADC size agreed with the maximum radius for hydrostatic equilibrium if we assume $kT = 44$ keV (Church 2001) supporting this higher temperature. The present result from curve of growth analysis that the ion types are consistent with a $kT \sim 45$ keV thus suggest that the absorption lines are formed in the accretion disc corona, and we propose that the ADC is the site of absorption line production in all the dipping LMXB.

Conditions in the ADC are not well understood, and the formation of the ADC has also not been understood, with theoretical models divided between intrinsic processes such as disc instabilities and external models in which irradiation of the disc by the central source leads to formation. Our results demonstrating the very extended nature of the ADC support the irradiation models (e.g. Jimenez-Garate, Raymond & Liedahl et al. (2002); Rózańska & Czerny 1996). These models show that above the disc will be an atmosphere or boundary layer, with a hot, less dense corona above this. The ADC temperature is less than 10 keV; however, this is not totally consistent with X-ray spectra of sources such as XB 1916-053 and XB 1323-619 (Church 2001) where the cut-off energies are high (81 keV and 44 keV, respectively) showing that kT_e can be 25 keV or more. Jimenez-Garate et al. provide calculations of proton density as a function of height above the disc, with values of up to 10^{14} cm^{-3} at a radius of the outer ADC (10^{10} cm; Church & Bałucińska-Church 2004). Assuming this to be constant, we estimate the column density for a path length of 10 percent of this as $\sim 10^{23}$ atom cm^{-2} , i.e. relatively similar to the level of $\sim 10^{24}$ atom cm^{-2} implied by the Fe absorption lines in this work.

The formation of the ADC in illumination models takes place initially as a hot skin which is evaporated from the accretion disc. The models assume that energy is absorbed from the central X-ray source and then redistributed vertically to produce a distribution of plasma density and temperature. Thus it is likely that the ion distribution in the ADC will depend on collisional ionization at the ADC temperature, and is not produced by photo-ionization in the ADC itself.

In deep dipping, the Fe XXV K_{α} absorption line is stronger than in the non-dip spectrum. The normalization of the line in the dip spectra is ~ 5 times larger than in non-dip,

while the continuum at this energy is reduced by a factor of two compared with non-dip. This clearly shows that there is a concentration of Fe XXV ions in the bulge in the outer disc resulting in increased depth of the absorption line. However, the line energy is reduced compared with non-dip showing that the ionization state is not so high as for the absorber producing the line in non-dip emission. The reduced quality of the dip spectra make it difficult to get accurate equivalent widths and thus accurate ratios for the ions Fe XXVI and Fe XXV, so that a detailed numeric evaluation of column densities is not sensible. However, for an approximate EW of 100 eV for Fe XXV, N_{FeXXV} is $\sim 10^{20}$ ion cm^{-2} and the hydrogen column density N_{H} must be at least 10^{24} atom cm^{-2} . Such values are not inconsistent with column densities in the bulge in the outer disc as revealed from dip spectra.

Finally, we comment on the remarkable linear increase in the rate of X-ray bursting which we show has continued unchanged over an 14 year period. This predicts that the gap between bursts would become zero on Jan 11, 2008. However, we do not expect the behaviour of the source to continue unchanged till then, since as the luminosity increases further in the band 10^{37} to 10^{38} erg s^{-1} , we expect the source to change from a bursting source to a flaring source, since bursts are not generally seen from high luminosity sources. Observation during this period will be very interesting allowing investigation of the transition. The observation of a smooth transition between bursting and flaring would clearly support the origin of flares as unstable nuclear burning as proposed theoretically (e.g. Bildsten 1995).

ACKNOWLEDGMENTS

This work was supported in part by the Polish KBN grant KBN-1528/P03/2003/25

REFERENCES

- Angelini L., Church M. J., Parmar A. N., Bałucińska-Church M., Mineo T., 1998, A&A, 339, L41
- Bałucińska-Church M., Church M. J., Oosterbroek T., Segreto A., Morley R., Parmar A. N., 1999, A&A, 349, 495
- Bałucińska-Church M., Barnard R., Church M. J., Smale A. P., 2001, A&A, 378, 847
- Barnard R., Bałucińska-Church M., Smale A. P., Church M. J., 2001, A&A, 380, 494
- Barnard R., Church M. J., Bałucińska-Church M., 2003, A&A, 405, 237
- Bildsten L., 1995, ApJ, 438, 875
- Boirin L., Parmar A. N., Barret D., Paltani S., Grindlay J. E., 2004a, A&A, 418, 1061
- Boirin L., Méndez M., Díaz Trigo M., Parmar A. N., Kaastra J. S., 2004b, A&A, submitted
- Church M. J., 2001, Adv Space Res, 28, 323
- Church M. J., Bałucińska-Church M., 1993, MNRAS, 260, 59
- Church M. J., Bałucińska-Church M., 1995, A&A, 300, 441
- Church M. J., Bałucińska-Church M., 2001, A&A, 369, 915
- Church M. J., Bałucińska-Church M., 2004, MNRAS, 348, 955

- Church M. J., Mitsuda K., Dotani T., Bałucińska-Church M., Inoue H., Yoshida K. 1997, *ApJ*, 491, 388
- Church M. J., Bałucińska-Church M., Dotani T., Asai K., 1998a, *ApJ*, 504, 516
- Church M. J., Parmar A. N., Bałucińska-Church M., Oosterbroek T., Dal Fiume D., Orlandini M., 1998b, *A&A*, 338, 556
- Courvoisier T. J.-L., Parmar A. N., Peacock A., Pakull M., 1986, *ApJ*, 309, 265
- Forman W., Jones C., Cominsky L, Julien P., Murray S., Peters G., Tannanbaum H., Giacconi R., 1978, *ApJS*, 38, 357
- Galloway D. K., Cumming A., Kuulkers E., Bildsten L., Chakrabarty D., Rothschild R. E., 2004, *ApJ*, 601, 466
- Gierliński M., Done C., 2002, *MNRAS*, 337, 1373
- Jimenez-Garate M. A., Raymond J. C., Liedahl D. A., 2002, *ApJ*, 581, 1297
- Kallman T. R., McCray R., 1982, *ApJS*, 50, 263
- Kotani T., Ebisawa K., Dotani T., Inoue H., Nagase F., Tanaka Y., Ueda Y., 2000, *ApJ*, 539, 413
- Oosterbroek T., Parmar A. N., Sidoli L., in't Zand J. J. M., Heise J., 2001, *A&A*, 376, 532
- Makishima K., 1986, The physics of accretion onto compact objects, Proc. of Tenerife workshop, 1986, Lecture Notes in Physics, 266, Springer-Verlag, p249
- Parmar A. N., White N.E., Giommi P., Gottwald M., 1986, *ApJ*, 308, 199
- Parmar A. N., Gottwald M., van der Klis M., van Paradijs J., 1989, *ApJ*, 338, 1024
- Różańska A., Czerny B., 1996, *Acta Astron*, 46, 223
- Sidoli L., Parmar A. N., Oosterbroek T., Stella L., Verbunt F., Masetti N., Dal Fiume D., 2001, *A&A*, 368, 451
- Smale A. P., Mason K. O., White N. E., Gottwald M., 1988, *MNRAS*, 232, 647.
- Smale A. P., Church M. J., Bałucińska-Church M., 2001, *ApJ*, 550, 962
- Smale A. P., Church M. J., Bałucińska-Church M., 2002, *ApJ*, 581, 1286
- Stark A. A., Gammie C. F., Wilson R. W., et al., 1992, *ApJS*, 79, 77
- Strohmayer T., Bildsten L., 2003, in *Compact Stellar X-ray Sources*, eds W. H. G. Lewin, M. van der Klis, Cambridge
- Ueda Y., Asai K., Yamaoka K., Dotani T., Inoue H., 2001, *ApJ*, 556, L87
- Van der Klis M., Jansen F., van Paradijs J., Stollman G., 1985, *Space Sci Rev*, 30, 512
- Walter F. M., Mason K. O., Clarke J. T., Halpern J., Grindlay J. E., Bowyer S., Henry J. P., 1982, *ApJ*, 253, L67
- Warwick R. S., Marshall N., Fraser G. W., et al., 1981, *MNRAS*, 197, 865
- White N. E., Swank J. H., 1982, *ApJ*, 253, L61